ACS OMEGA

Article

Cite This: ACS Omega 2019, 4, 13631−13639

http://pubs.acs.org/journal/acsodf

Sonochemical One-Step Synthesis of Polymer-Capped Metal Oxide Nanocolloids: Antibacterial Activity and Cytotoxicity

Anjani P. Nagvenkar,[†] Ilana Perelshtein,[†] Ylenia Piunno,[‡] Paride Mantecca,[‡] and Aharon Gedanken*[,†]

[†]Department of Chemistry and Institute for Nanotechnology and Advanced Materials, Bar-Ilan University, Ramat-Gan 5290002, Israel

[‡]Department of Earth and Environmental Sciences, Research Center POLARIS, University of Milano-Bicocca, Milan 20126, Italy

Supporting Information

ABSTRACT: Most antibacterial agents demand their action in the form of a liquid for compatibility and ease of use in biosystems, which are mainly composed of biological fluids. Controlling the colloidal stability of metal oxide nanocolloids, in parallel with minimizing the effect of using a large amount of surfactant on their biocidal activity and cytotoxicity, remains a challenge. Here, we address the stability of nanocolloids of ZnO and CuO in the presence of polymer surfactants and the influence of the surface capping on their antibacterial activity and cytotoxicity. The metal oxide nanoparticles (NPs) were synthesized sonochemically in a single step and tested against both Gram-negative *Escherichia coli* and Gram-positive *Staphylococcus aureus* to validate their biocidal efficacy. Cytotoxicity studies were performed on human alveolar epithelial cells. Polyethylene glycol- and polyvinyl alcohol-capped NPs are observed to show the minimum cytotoxicity whereas polyethylene imine-capped and pristine metal oxide NPs are toxic to the mammalian cells. The cytotoxic and antibacterial properties of the stable nanocolloids displayed an inverse relation, highlighting the role and significance of the polymer capping. The nontoxic biocidal nanocolloids showed an effective antibacterial efficacy of 99.9% in 2 h.

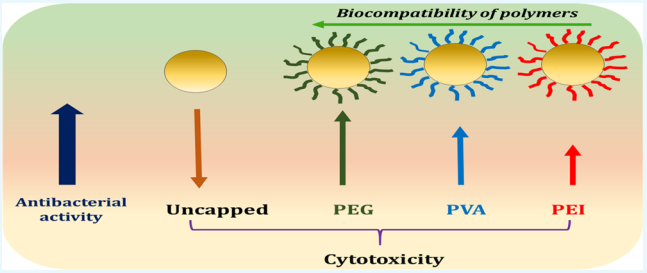

INTRODUCTION

Metal oxides are the most explored class of inorganic materials owing to their unique physical and chemical properties, controllable particle size, low synthesis cost, and high stability.[1] The use of metal oxide nanoparticles (NPs), termed MONPs, has drawn immense attention in the biomedical field as a result of their biocompatibility, comparatively low toxicity, and reduced bacterial resistance.[2−4] Their role as biocidal agents flourished, as they are considered biologically benign materials, which are relatively less hazardous to the environment and human health. CuO and ZnO, being constituted by essential elements, are more biocompatible than other metal oxides and their toxicity is lower than, for example, silver- or nickel-based NPs. However, the presence of heavy elements raises the issues of cytotoxicity of these MONPs at higher concentrations. In addition, the stability of the NPs toward agglomeration is an important concern from the point of its applicability.[5−8] Considering the primary issue of stability, the profound effect of the size of the NPs on the antibacterial activity of the MONPs renders importance to the stability of the NPs in solution.[9] The use of a surfactant or capping agent proved to significantly prolong the lifespan of NPs in suspension by avoiding agglomeration.[10,11] In addition, during synthesis, the presence of surfactant molecules in the reaction cell leads to the formation of smaller NPs, as nucleation occurs in the surfactant matrix, with immediate capping of the NPs by surfactant molecules, preventing further growth.

The cytotoxic nature of MONPs is also a matter of concern because of their potential effects on the human health and the environment.[12,13] Reactive oxygen species (ROS) are considered the primary mechanistic pathway for the cellular oxidative stress resulting in biocidal activity of MONPs, and are therefore used to determine the level of toxicity.[14] The current work focuses on both issues by synthesizing colloidal solutions of metal oxides in the presence of polymers as surfactants and studying their biocidal and cytotoxic properties. As most biological processes occur in an aqueous environment, the application of MONPs in the suspended colloidal form is crucial for better assimilation and functioning of these agents in biosystems. Colloidal solutions of NPs, termed nanocolloids, are thus most suitable for biological fluids. In order to achieve nanocolloids with higher stability and a homogenous dispersion of NPs, ultrasound-assisted synthesis was found to be an effective technique.[4] Although nanocolloids of CuO and ZnO are widely exploited in varied areas of nanoscience, their application as antibacterial agents in the colloidal form was seldom explored.[15−18] Khashan et al. tested the antibacterial

Received: January 20, 2019
Accepted: March 21, 2019
Published: August 12, 2019

DOI: 10.1021/acsomega.9b00181
ACS Omega 2019, 4, 13631−13639

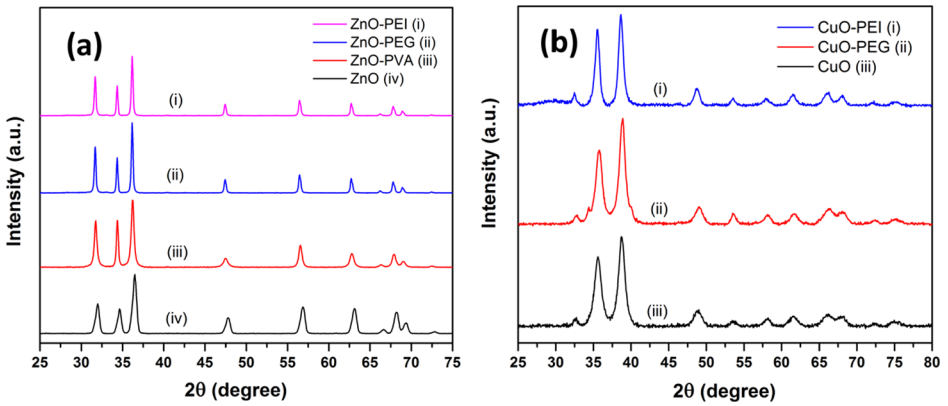

Figure 1. Representative XRD profiles of (a) ZnO-capped with (i) PEI, (ii) PEG, and (iii) PVA and (iv) pristine and (b) CuO-capped with (i) PEI (ii) PEG, and (iii) pristine.

activity of CuO suspension prepared by laser ablation of the copper metal pellet and reported a synergistic effect of the CuO NPs with the antibiotic amoxicillin.[19] Mahapatra et al. prepared a CuO suspension by dispersing the as-synthesized CuO NPs in water in the absence of surfactants and conducted antibacterial and cytotoxicity studies.[20] To our knowledge, there are no reports in the literature of antibacterial and cytotoxicity assays conducted on stable CuO/polymer nanocolloids with CuO NPs fabricated in situ in the polymer matrix using ultrasonication. In the case of ZnO, despite countless reports on its antibacterial activity, only recently the biocidal properties were collated by our group following a one-step synthesis of colloidal ZnO by the sonochemical method,[28] providing the highest stability of ZnO NPs reported so far.

Many studies addressed the toxic effects of CuO and ZnO NPs, suggesting possible hazardous effects in humans and other organisms.[21] Although a large amount of toxicity data was collected, a debate is still open about the properties of these MONPs, in particular regarding their biological reactivity and adverse outcome pathways that are evoked. The size and shape of the NPs, as well as their crystalline structure, significantly influence the toxic behavior. Smaller and round-shaped ZnO NPs tend to display higher toxicity than bigger and rod-shaped particles.[22,23] Similarly, for CuO NPs, the small size of the particles was pointed out as a main driver of cell toxicity, determining both higher bioavailability and enhanced intracellular reactivity, finally determining significant cytotoxic and genotoxic effects.[24−26] In a previous study, we investigated not only the antibacterial efficacy but also the cytotoxic properties of differently synthesized CuO and ZnO NPs, which were observed to depend on the size and shape and, perhaps even more interestingly, on their crystalline structure.[27]

The adverse effects of MONPs on nontarget cells and organisms vary according to the modalities by which the NPs interact with the biological systems; for example, size, shape, and agglomeration are able to modulate differently the endocytosis mechanism.[28] At the same time, the protein corona effect can be modulated by the NP physicochemical characteristics as well as by the medium in which NPs are dispersed.[29] Doped or coated MONPs were seen to induce different toxicities in human cells, and it was put in relation to the decreased dissolution or to the more or less bioavailability, according to the surface identity acquired by the NPs.[30] These modalities change according to the physicochemical properties of the NP, and today there is very active investigation aimed at lowering the adverse biological effects of MONPs by controlling the influencing factors, for example, the NP size, shape, and surface properties. Toxicity and biocompatibility studies on polymer-capped MONPs are therefore of high relevance.

The current study reports the first attempt, to the best of our knowledge, to synthesize MONP colloids by a facile one-step sonochemical method and concomitantly characterize their biological activity. Stability issues in the formed suspensions are obviated by using optimal amounts of polymer that serves as the capping agent. The surfactant-stabilized nanocolloids are compared with their pristine MONP counterparts, and the biocidal properties are discussed, along with the aspects related to the toxicity.

RESULTS AND DISCUSSION

Optical and Morphological Characterization. The surfactant-stabilized synthesis of ZnO and CuO nanocolloids was achieved in a single step using the well-established ultrasound technique.[31] Three water-soluble surfactants were used—polyvinyl alcohol (PVA), polyethylene glycol (PEG), and polyethylenimine (PEI) in different weight ratios with respect to the precursor metal acetate. As the stability of a colloid grows with the amount of the capping agent surrounding the NP in the liquid matrix, a substantial amount of surfactant was used to impart maximal stability to the synthesized colloids; weight ratios of the surfactant to metal acetate were optimized, as mentioned in Table S1. Increasing the amount of surfactant above 30 wt % with respect to the metal salt precursor hindered complete formation of MONPs in the matrix. This was evidenced by the appearance of a translucent turbid liquid after addition of ammonia instead of opaque white (ZnO) or dark brown (CuO) colored colloids, indicating an incomplete reaction. The formation of CuO was not achieved in the PVA matrix because of the formation of a green-colored Cu(II)−PVA complex,[32,33] which inhibited the hydrolysis of Cu^{2+} ions in the solution. As shown in Table S1, the amount of PEI is restricted to 5 wt % because of its basic nature, which raises the pH of the solution above 9. This leads to dissolution of the as-formed metal oxide NPs, impeding formation of a nanocolloid.

The crystallinity and structure of the synthesized metal oxides with different surfactants were analyzed by X-ray diffraction (XRD) (Figure 1). The peaks of ZnO and CuO correspond to the planes of hexagonal zincite and monoclinic tenorite, respectively, and match the Joint Committee for

DOI: 10.1021/acsomega.9b00181
ACS Omega 2019, 4, 13631−13639

Powder Diffraction Studies (JCPDS) files no. 70-2551 and 41-0254, respectively. The bulk amount of polymer in the reaction mixture did not affect the crystallinity of the NPs. The formation of ZnO and CuO NPs in the polymer matrix was further confirmed by recording UV−vis absorption spectra (Figure S1). The pristine ZnO shows an absorption peak at 364 nm, while the surfactant-capped NPs exhibit peaks at lower wavelengths, indicating smaller particles. ZnO−PVA displayed absorption peaks at 344 and 357 nm, ascribed to ZnO NPs and ZnO−PVA complex, respectively.[31] Similarly, absorption peaks at 346 and 361 nm were observed for ZnO−PEG and ZnO−PEI, respectively; the higher absorption wavelength of the latter, indicating larger particles, can be imputed to the significantly lower amount of surfactant used. UV−vis spectra of the CuO colloids revealed a broad absorption region centered at 298, 287, and 276 nm for CuO, CuO−PEG, and CuO−PEI, respectively (Figure S1). Thus, we can state that the blue shift in the absorption spectra of the polymer-capped NPs with respect to their pristine forms affirms that NPs with a smaller average size were formed in the presence of the capping agent.

The stability of the NPs in the colloid can be estimated from the zeta potentials, which assess the surface charge on the nanoparticle. Higher zeta potentials imply increased charge, and thus stronger electrostatic repulsion, preventing the colloidal NPs from coming in contact with each other and minimizing agglomeration. The zeta potentials of the polymer-capped ZnO and CuO NPs are depicted in Figure 2. The lower values observed for the PEI-capped NPs imply that they are less stable. ZnO−PEG and CuO−PEG exhibited good stability over a period of 40 days, compared to the other surfactant-stabilized nanocolloids, in agreement with the zeta potentials observed for these samples. The pristine ZnO and CuO NPs synthesized in the absence of surfactant agglomerate and precipitate within 1 h of sonication.

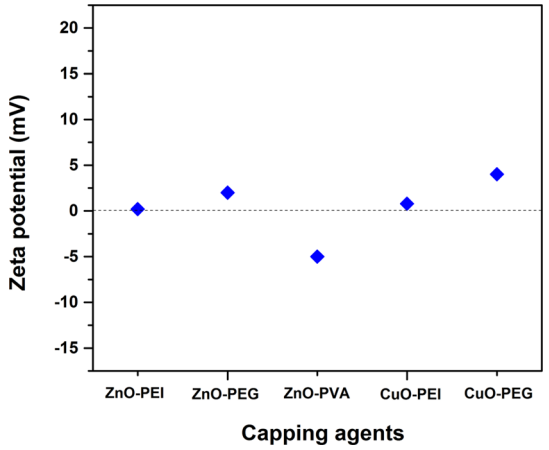

Figure 2. Zeta potentials for polymer-capped ZnO and CuO NPs.

Antibacterial Activity and Mechanism. The antibacterial properties of the polymer-capped ZnO and CuO nanocolloids are demonstrated against two types of bacterial strains: *Escherichia coli* (Gram-negative) and *Staphylococcus aureus* (Gram-positive). The killing kinetics for both strains of bacteria were monitored by the culturing (CFU/mL) method. The biocidal activity of the synthesized nanocolloids (tested at a concentration of 0.5 mg/mL) is represented in Figures 3 and 4. For *E. coli*, CuO−PEG and ZnO−PVA demonstrated 99.9% bacterial killing after 120 min of exposure, while CuO−PEI and ZnO−PEG were less active. ZnO, ZnO−PEI, and CuO showed 1, 1, and 2 log reduction, respectively, after 180 min exposure to the bacteria. Similarly, for *S. aureus*, CuO−PEG showed complete reduction after 120 min, whereas the same was observed for ZnO−PVA and CuO−PEI after 180 min of exposure. ZnO, CuO, and ZnO−PEI were found to exhibit lower antibacterial efficacy. The higher resistance of *S. aureus*, compared with *E. coli*, is ascribed to the thick peptidoglycan layer in the cell wall of *S. aureus*, making it less susceptible to the action of the MONPs.[34,35] Therefore, the observed higher antibacterial activity of CuO than ZnO was also validated previously and is in accordance with the present study.[36]

The most plausible mechanism for the effective biocidal activity of the metal oxides is believed to be the generation of ROS, which are a class of free radical species of oxygen.[37,38] These strong oxidants cause oxidative stress in the cell, damaging the cellular components and leading to cell disruption and death.[39] Assuming that a similar mechanism is responsible for the activity observed, correlation between generated ROS and the particle size of the NPs is developed. Electron spin resonance (ESR) is a widely used tool for detection of free radicals, in particular for measurement of ROS using 5,5-dimethyl-1-pyrroline-*N*-oxide (DMPO) as a spin trap.[40] DMPO captures $^{\bullet}$OH and superoxide anions, giving a quadrant signal arising from DMPO-OH and DMPO-OOH, respectively. Using equal concentrations of DMPO and the samples, comparison is based on the intensity of the quartet signal. The higher the signal intensity, the higher is the production of ROS by the NP. Figure 5 presents the quartet

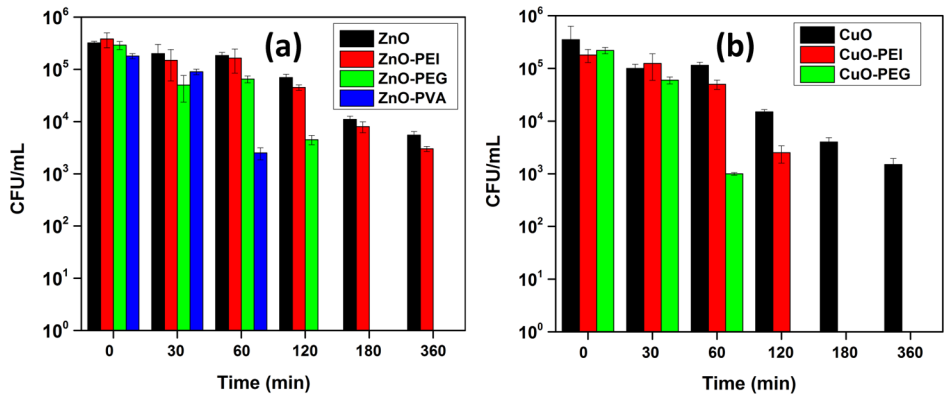

Figure 3. Antibacterial activity of pristine and surfactant-stabilized nanocolloids of (a) ZnO and (b) CuO against *E. coli*.

DOI: 10.1021/acsomega.9b00181
ACS Omega 2019, 4, 13631−13639

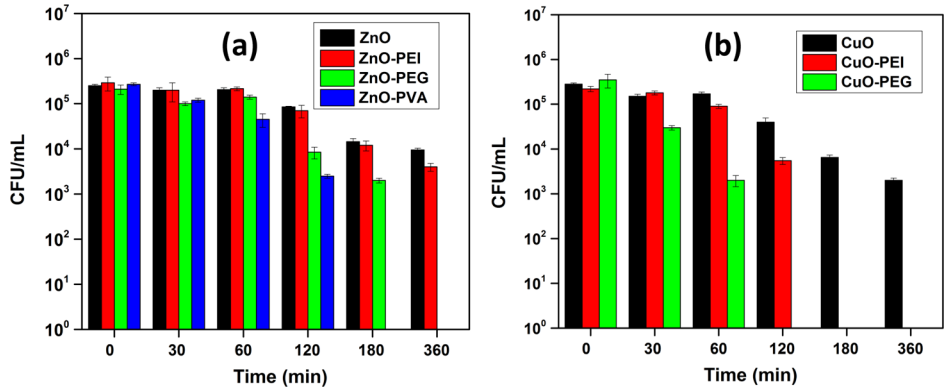

Figure 4. Antibacterial activity of pristine and surfactant-stabilized nanocolloids of (a) ZnO and (b) CuO against *S. aureus*.

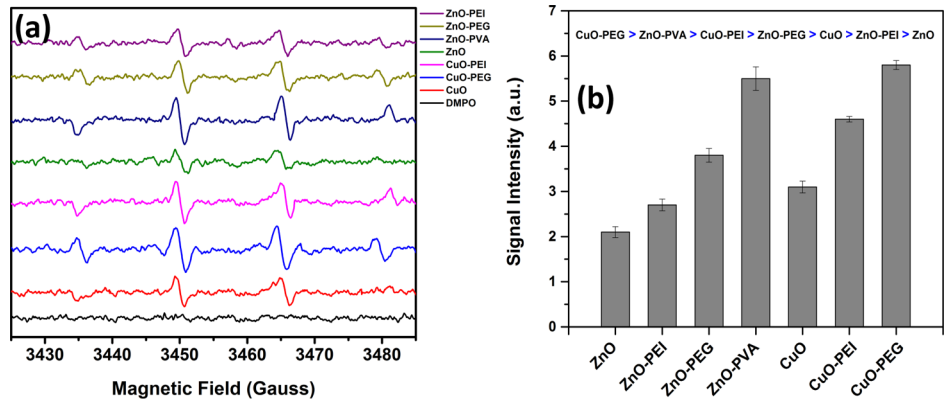

Figure 5. ESR spectra demonstrating (a) relative ROS production by ZnO and CuO NPs in the surfactant matrix and (b) integrated area depicting signal intensity of the generated ROS.

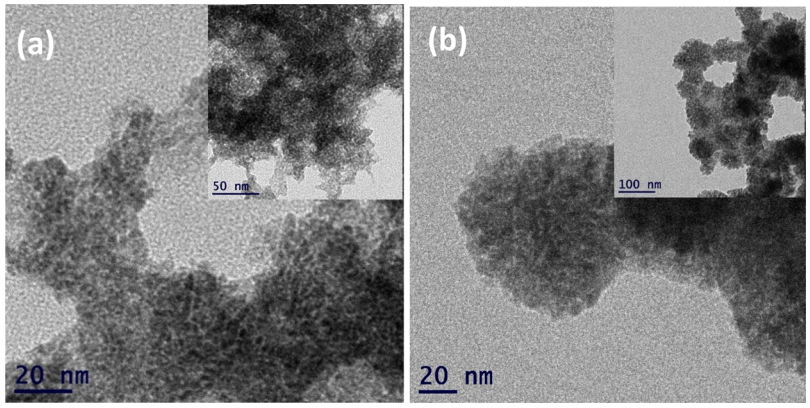

Figure 6. TEM images of the colloidal NPs: (a) CuO−PEG and (b) ZnO−PVA. Inset shows the low magnification images of the samples.

ESR signals and signal intensities of the ROS generated by the nanocolloids. The relative amounts of ROS produced by the samples are: CuO−PEG > ZnO−PVA > CuO−PEI > ZnO−PEG > CuO > ZnO−PEI > ZnO. The ESR results favor the biocidal activity rendered by the capped metal oxide colloids, wherein higher ROS accounts for faster killing of the bacteria by the nanocolloid. Thus, the bacterial survival rate is observed to decrease with the increase in total ROS concentration.

Having affirmed that the expected mechanism of ROS generation is indeed responsible for the effective antibacterial potency of the nanomaterials, the source and enhancement in its production are further elucidated in detail. The primary source of ROS formation is the presence of lattice defect sites in the nanomaterial; these sites serve as active spots for adsorption of water molecules and their dissociation, generating oxygen radicals.[27,41] The present study in which metal oxide nanocolloids were synthesized using ultrasound supports this finding. The acoustic energy from the sonication process during nucleation of the metal oxide crystal introduces defects and dislocations, yielding a highly perturbed nanocrystal.[31,42] The size of the NP also has a profound effect on the amount of ROS generated by the nanomaterial. Compared to the bulk particle, the NP has a higher surface area and thus higher surface reactivity for ROS production.[43] The particle sizes of the NPs reported here, along with the ESR signal intensity of the ROS, are in accordance with the observed

DOI: 10.1021/acsomega.9b00181
ACS Omega 2019, 4, 13631−13639

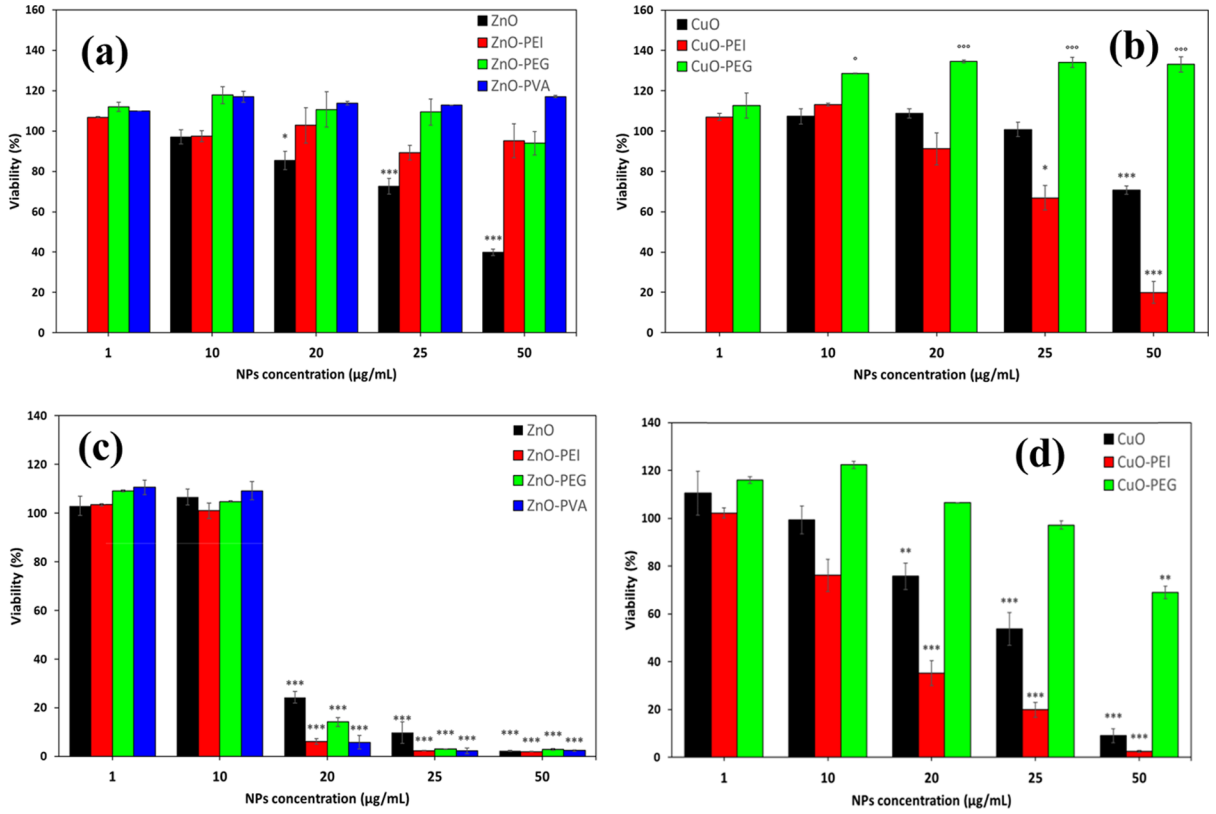

Figure 7. Cytotoxicity of pristine and surfactant-stabilized nanocolloids. Cell viability was measured by the [3-(4,5-dimethylthiazol-2-yl)-2,5-diphenyltetrazolium bromide] MTT assay. (a,b) Effects of ZnO and CuO NPs after 3 h exposure and (c,d) effects of ZnO and CuO NPs after 24 h exposure.

bactericidal efficiency of these nanocolloids. A Table S2 summarizes the average particle sizes and the corresponding zeta potential values. The lowest particle sizes of ∼6 and ∼7 nm are displayed by CuO−PEG and ZnO−PVA, respectively (Figures 6 and S2). These samples indeed show the highest ROS production and clearly exhibit the best antibacterial efficacy among the NPs. Pristine ZnO and CuO, without stabilizing agents, have the largest particle size, which might be responsible for their reduced antibacterial activity.

Cytotoxicity of the Nanocolloids. Cytotoxicity was measured in human A549 cells exposed to the colloidal ZnO and CuO NPs for 3 and 24 h; results are shown in Figure 7. It is clear that with the exception of CuO−PEI, which revealed higher toxicity than pristine CuO, all colloidal ZnO and CuO NPs are less cytotoxic than the corresponding pristine NPs after both 3 h (Figure 7a,b) and 24 h (Figure 7c,d).

The polymer capping of the ZnO NPs resulted in less effective modulation of the cytotoxicity, as after 24 h exposure all ZnO nanocolloids were strongly cytotoxic at concentrations ≥20 ppm, while no effects were measured for pristine and surfactant-capped ZnO exposure to ≤10 ppm (Figure 6c). After 3 h of exposure, the ZnO nanocolloids demonstrated lower cytotoxicity with respect to pristine ZnO (Figure 6a); it is noteworthy that ZnO−PVA did not induce any decrease in cell viability even at the highest concentration tested, confirming PVA capping as the most promising approach for safer ZnO NPs.

Regarding CuO, stabilization with PEI conferred an augmented cytotoxic potential to the NPs, as demonstrated by the significant and concentration-dependent decrease in cell viability at both 3 and 24 h exposures (Figure 6b,d). On the contrary, CuO−PEG was only slightly cytotoxic, as a significant decrease in cell viability was observed only after 24 h exposure at very high (50 ppm) concentration (Figure 6d). After 3 h, pristine CuO was already cytotoxic, while CuO−PEG was not, and during the 3 h, it even induced a slight increase in cell metabolism (Figure 6b). After 24 h exposure, the cytotoxicity of CuO was significantly rescued by PEGylation (Figure 6d), as cell viability did not significantly decrease even with respect to the control until the highest exposure concentration of 50 ppm.

From the toxicity studies, we can conclude that the polymer stabilization of the NP suspensions was very effective in modulating the cytotoxic properties of CuO, while for ZnO it was less effective. PEI coating makes the CuO NPs more cytotoxic, while PEGylation renders them safer.

Comparison between the Cytotoxicity and Antibacterial Results. Decreasing antibacterial activity due to decreased ROS generation

CuO−PEG > ZnO−PVA > CuO−PEI > ZnO−PEG > CuO > ZnO−PEI > ZnO

Decreasing cytotoxicity after 3 h at 25 ppm concentration (increasing cell viability)

CuO−PEI > ZnO−PEI > ZnO−PEG > ZnO−PVA > CuO−PEG

Decreasing cytotoxicity after 24 h at 25 ppm concentration (increasing cell viability)

ZnO−PEI > ZnO−PEG > ZnO−PVA > CuO−PEI > CuO−PEG

The higher cytotoxicity of the MONPs with PEI as the surfactant is in accordance with the significantly lower amount

DOI: 10.1021/acsomega.9b00181
ACS Omega 2019, 4, 13631−13639

of surfactant used, leading to increased exposure of the NPs to the cell surface. Moreover, PEI was recognized as an agent that promotes cell penetration and is commonly used as a gene delivery agent owing to its high transfection efficiency; it is also known to interact with the negatively charged cell surface, promoting its attachment to the cell and cell uptake.[44,45] The fact that at 3 h of exposure, PEI is able to enhance the cytotoxic properties of CuO NPs but not those of ZnO NPs can be justified by the following claim. According to the proton-sponge effect, it can induce a lysosomal escaping effect, which finally may determine an increase of MONPs free in the cytoplasm, where they can induce oxidative damages to the intracellular membrane systems. It was demonstrated that in the water aqueous environment, sonochemically synthesized CuO NPs produce more ROS than ZnO NPs. If in the presence of PEI, they are released from the endolysosomal compartments, without massive dissolution (and it likely occurs during short-term exposure, e.g. 3 h), CuO NPs may induce higher oxidative damages to protein and lipid membrane domains, culminating in a significant decrease in cell viability. At prolonged exposure time (24 h), the extracellular and intracellular dissolution of CuO and ZnO NPs become the main determinant of the induced toxicity, masking the effect of the polymers used. This is particularly relevant for ZnO NPs, which dissolve easier than CuO ones, ending up in comparable cytotoxic effects of ZnO colloidal suspensions produced with the different polymers. However, the speculations need additional experimental evidences to be proved and are of interest for future study. The novel nanomaterial CuO−PEI, which combines the high surface reactivity of the CuO NPs with the unique properties of the PEI surface coating, could potentially be useful in selective killing of human cells undergoing uncontrolled proliferation.

Regarding the safety of the antibacterial metal oxide nanocolloids, the results highlight CuO−PEG as the most promising material capable of preserving cell viability, followed by ZnO−PVA.

It is interesting to note that, with the exclusion of the PEI-capped NPs, the cytotoxicity follows an inverse relation with the antibacterial activity and ROS generation capacity of the MONPs in a cell-free environment. To explain these interesting experimental results, more research on the toxicity mechanisms in both bacterial and human cells is required.

At the moment, based on the literature, we can speculate that PEG surface coating of the CuO NPs could have influenced their cellular internalization and successive intracellular reactivity. It is known that PEG functional coating of different NPs determines their cellular uptake and internalization.[46,47] In addition, on account of its biocompatibility, PEGyaltion of NPs is a reported strategy to minimize the nanotoxicity of the particles, with diminished impact on cell viability. This is because PEG on the surface prevents the particle opsonization by the proteins present in the body fluids or in the cell culture media, which has been seen to enhance NP uptake by receptor-mediated endocytosis (thus preventing phagocytosis by specialized immune cells).[48] Hence, also in the present work, PEGylation may have determined a lower internalization of CuO NPs in human cells, justifying the low toxicity even in the presence of highly reactive NPs. On the contrary, it is demonstrated that the mechanism at the base of the antibacterial activity of CuO NPs is related to the contact at the cell surface level and the consequent oxidative stress leading to the cell death. Together with the high capability of mammalian cells to efficiently buffer oxidative stress by a complex intracellular enzymatic system,[49,50] the current results may justify the increased safety of CuO−PEG toward mammalian cells, while being strongly toxic toward bacterial cells.[51,52]

The less effective results achieved with polymer coating of ZnO NPs, including PEGylation, with respect to CuO NPs, may be attributed to the different cytotoxic mechanism of these two metal oxides. For CuO, a significant role in the toxicity toward mammalian cells is played by the particle surface reactivity—PEGylated CuO showed the lowest cytoxicity, followed by the PEI-coated and pristine CuO NPs. For ZnO, on the other hand, a major role was attributed to the Zn ion dissolution both extra- and intracellularly.[53] The intracellular dissolution of the ZnO NPs, which determines the cytotoxicity of the ZnO, increases with the concentration of the NPs and shows a profound effect at concentrations higher than 10 μg/mL.[54] The solubility product constant (K_{sp}) of CuO is around 10^{-22} at room temperature, meaning that there are effectively no ions of Cu^{2+} in the solution (the concentration of Cu ions is 10^{-11} M). On the other hand, the K_{sp} of ZnO is much higher—around 10^{-10}, yielding 10^{-5} mol per liter of Zn^{2+}. This significant solubility could explain the higher cytotoxicity of ZnO.

CONCLUSIONS

In conclusion, we have demonstrated antibacterial and cytotoxic studies conducted on stable ZnO and CuO nanocolloids synthesized using a high amount of surfactant. The sonochemical method reported is unique and feasible to scale up preparation of metal oxide nanocolloids for wide use as antibacterial agents. The present results confirm the crucial role of polymer capping in mitigating the effect of NPs on mammalian cells, while still exhibiting notable antibacterial effects. The current study also affirms the role and significance of the type of polymer used as the capping agent in deciding the overall cytotoxicity of the samples. PEI is observed to enhance toxicity, whereas PEGylation of the NPs reduces the toxic effect. Finally, solubility of the MONPs is a decisive factor in their cytotoxicity—ZnO is much more soluble than CuO, offering a plausible explanation of the higher toxicity of ZnO−PEG relative to CuO−PEG.

EXPERIMENTAL SECTION

Zn(II) acetate dihydrate, Cu(II) acetate monohydrate, poly(vinyl alcohol) (PVA) MW = 88−98 K, PEG MW = 6 K, and PEI branched 50% w/v in H_2O MW = 75 K were purchased from Sigma-Aldrich and used as received without further purification. The precursor salts and polymers were separately dissolved in deionized water. The two solutions were mixed together to obtain a total volume of 100 mL. The concentration of metal ions was maintained at 0.01 M, and the weight ratios of the metal acetate to polymer were 1:5 for Cu(acetate)·H_2O/PEI and Zn(acetate)·$2H_2O$/PEI and 1:30 for the rest. The obtained solution of metal ions with the dissolved polymer was irradiated with an ultrasonic probe (Tihorn@20 kHz, 100 W cm^{-2}). The temperature was allowed to rise, and upon reaching 60 °C, ∼0.2 mL of an aqueous solution of ammonium hydroxide (28−30%) was introduced into the reaction mixture to achieve a pH of ∼8. Completion of the reaction was indicated by color change—from colorless to white and from bluish-green to dark brown for ZnO and CuO,

DOI: 10.1021/acsomega.9b00181
ACS Omega 2019, 4, 13631−13639

respectively, confirming the formation of MONPs in the colloidal polymer matrix. Sonication was continued for 30 min, and the mixture was chilled in an ice bath to maintain a reaction temperature of 25 °C. Pristine ZnO and CuO in suspension were synthesized by following the same procedure in the absence of polymers.

Characterization. XRD patterns for ZnO and CuO were obtained using a Bruker D8 ADVANCE X-107 X-ray diffractometer using Cu Kα (λ = 1.5418 Å) as the source. Zeta potential was performed on a Nano ZS Malvern Zetasizer instrument. High-resolution transmission electron microcopy (HR-TEM) images were obtained using a JEOL JEM-2100 model operated at an accelerated voltage of 200 kV. The absorption spectrum of the ZnO−PVA nanofluid was recorded on a CARY Bio 100 spectrophotometer (Varian, Australia). The metal oxide concentration in the colloid was determined by inductively coupled plasma analysis. The amount of generated ROS was determined by ESR using a 121 Bruker EPR 100d X-band spectrometer with DMPO as a spin trap. To 80 μL of the colloidal sample, 20 μL of DMPO (0.01 M) was added, and the solution was drawn by a syringe into a gas-permeable Teflon capillary. The capillary was folded twice, inserted into a narrow quartz tube open at both ends, and placed in the ESR cavity. The blank was measured by replacing the sample with deionized water.

Antibacterial Assay. The antibacterial activities of the synthesized metal oxide colloids with different capping agents were tested against two common strains of bacteria, namely Gram-negative *E. coli* and Gram-positive *S. aureus*. The antibacterial activity of these different nanocolloids was investigated using the colony-forming units per mL (CFU/mL) method. Strains of both bacteria were aerobically grown by incubating overnight at 37 °C in Luria Bertani (LB) broth. Following incubation, 0.2 mL aliquots were transferred to 10 mL of fresh LB broth and incubated at 37 °C for a further 3 h. The culture was further diluted 3-fold in LB broth to yield a bacterial suspension with a density of 10^5 CFU/mL. Time-kill experiments were conducted by adding 500 μL of nanocolloid solution (0.5 mg/mL) to 500 μL of bacterial suspension. The suspensions were shaken on a rotary shaker at 200 rpm and simultaneously incubated at 37 °C. After every 30 min, 100 μL aliquots were taken from each sample, diluted 10-fold in 10% LB medium, and transferred to nutrient agar plates. The plates were incubated at 37 °C for 16 h and counted for viable bacteria.

Cytotoxicity. Aqueous NP suspensions used for cytotoxicity studies were obtained by diluting the stock colloidal suspensions in the cell culture medium to obtain final concentrations of 1, 10, 20, 25, and 50 μg/mL of ZnO and CuO. The suspensions of pristine ZnO and CuO were obtained by diluting the NP powders in ultrapure (MQ) water to obtain stock suspensions of 2 mg/mL, which were sonicated for 30 min in an ultrasonic bath (Sonica Ultrasonic Extractor, Soltec, Italy). Aliquots from the stock solution were prediluted in MQ water (20-fold intermediate stock solution of NPs) and added to microplate wells containing serum-free OptiMEM medium to achieve the same NP test concentrations used for the colloidal suspensions.

The cell viability assay was performed following routine procedures established in our lab, as reported by Moschini et al.[25] Human alveolar epithelial cells, ATCC A549 (American Type Culture Collection), were routinely maintained in culture. For cell viability assays, cells were seeded (8×10^5) in six multiwell plates and exposed to NP suspensions for 3 and 24 h. Untreated cells were used as the control. At the end of treatments, cells were rinsed, and MTT [3-(4,5-dimethylthiazol-2-yl)-2,5-diphenyltetrazolium bromide] was added over 3 h to a final concentration of 0.0625 mg/mL in OptiMEM with 10% fetal bovine serum (FBS). The medium was removed, and the purple MTT reduction product (formazan crystals) was dissolved in DMSO. The absorbance of each sample, proportional to cell viability, was measured with a Multiskan Ascent multiplate reader spectrophotometer (Thermo Fisher Scientific Inc., USA) at 570 nm using 690 nm as the reference wavelength. Cell viability was expressed as OD mean percent (±SE). Statistical differences were tested by one-way ANOVA followed by Dunnett's test after evaluating the homogeneity of the variances among the treatment groups with the Levene test. Otherwise, for groups whose variances were found to be nonhomogeneous, statistical differences were tested with the Student's t-test followed by Bonferroni's test.

■ ASSOCIATED CONTENT

Supporting Information

The Supporting Information is available free of charge on the ACS Publications website at DOI: 10.1021/acsomega.9b00181.

UV visible spectra and TEM images of the metal oxide nanocolloids, and tables of weight ratio, zeta potential, and particle size (PDF)

■ AUTHOR INFORMATION

Corresponding Author

*E-mail: gedanken@mail.biu.ac.il.

ORCID

Paride Mantecca: 0000-0002-6962-049X

Aharon Gedanken: 0000-0002-1243-2957

Notes

The authors declare no competing financial interest.

■ REFERENCES

(1) Hahn, Y.-B.; Ahmad, R.; Tripathy, N. Chemical and Biological Sensors Based on Metal Oxide Nanostructures. *Chem. Commun.* **2012**, *48*, 10369−10385.

(2) Mamonova, I. A.; Babushkina, I. V.; Norkin, I. A.; Gladkova, E. V.; Matasov, M. D.; Puchin'yan, D. M. Biological Activity of Metal Nanoparticles and Their Oxides and Their Effect on Bacterial Cells. *Nanotechnol. Russ.* **2015**, *10*, 128−134.

(3) Yadavalli, T.; Shukla, D. Role of Metal and Metal Oxide Nanoparticles as Diagnostic and Therapeutic Tools for Highly Prevalent Viral Infections. *Nanomed. Nanotechnol. Biol. Med.* **2017**, *13*, 219−230.

(4) Stankic, S.; Suman, S.; Haque, F.; Vidic, J. Pure and Multi Metal Oxide Nanoparticles: Synthesis , Antibacterial and Cytotoxic Properties. *J. Nanobiotechnol.* **2016**, *14*, 1−20.

(5) Chen, J.; Zhu, J.; Cho, H.-H.; Cui, K.; Li, F.; Zhou, X.; Rogers, J.; Wong, S.; Huang, X. Differential Cytotoxicity of Metal Oxide Nanoparticles. *J. Exp. Nanosci.* **2008**, *3*, 321−328.

(6) Brayner, R.; Ferrari-Iliou, R.; Brivois, N.; Djediat, S.; Benedetti, M. F.; Fiévet, F. Toxicological Impact Studies Based on Escherichia Coli Bacteria in Ultrafine ZnO Nanoparticles Colloidal Medium. *Nano Lett.* **2006**, *6*, 866−870.

(7) Herman, D.; Walz, J. Y. Effects of Metal Oxide Nanoparticles on the Stability of Dispersions of Weakly Charged Colloids. *Langmuir* **2015**, *31*, 4844−4852.

DOI: 10.1021/acsomega.9b00181
ACS Omega 2019, 4, 13631−13639

(8) Li, C.-C.; Chang, M.-H. Colloidal Stability of CuO Nanoparticles in Alkanes via Oleate Modifications. *Mater. Lett.* **2004**, *58*, 3903−3907.
(9) Stankus, D. P.; Lohse, S. E.; Hutchison, J. E.; Nason, J. A. Interactions between Natural Organic Matter and Gold Nanoparticles Stabilized with Different Organic Capping Agents. *Environ. Sci. Technol.* **2011**, *45*, 3238−3244.
(10) Loosli, F.; Stoll, S. Effect of Surfactants, pH and Water Hardness on the Surface Properties and Agglomeration Behavior of Engineered TiO_2 Nanoparticles. *Environ. Sci.: Nano* **2017**, *4*, 203−211.
(11) Zaccone, A.; Wu, H.; Lattuada, M.; Morbidelli, M. Correlation between Colloidal Stability and Surfactant Adsorption/Association Phenomena Studied by Light Scattering. *J. Phys. Chem. B* **2008**, *112*, 1976−1986.
(12) Ajitha, B.; Kumar Reddy, Y. A.; Reddy, P. S.; Jeon, H.-J.; Ahn, C. W. Role of Capping Agents in Controlling Silver Nanoparticles Size, Antibacterial Activity and Potential Application as Optical Hydrogen Peroxide Sensor. *RSC Adv.* **2016**, *6*, 36171−36179.
(13) Granata, G.; Yamaoka, T.; Pagnanelli, F.; Fuwa, A. Study of the Synthesis of Copper Nanoparticles: The Role of Capping and Kinetic towards Control of Particle Size and Stability. *J. Nanopart. Res.* **2016**, *18*, 133.
(14) Kaweeteerawat, C.; Ivask, A.; Liu, R.; Zhang, H.; Chang, C. H.; Low-Kam, C.; Fischer, H.; Ji, Z.; Pokhrel, S.; Cohen, Y.; et al. Toxicity of Metal Oxide Nanoparticles in Escherichia Coli Correlates with Conduction Band and Hydration Energies. *Environ. Sci. Technol.* **2015**, *49*, 1105−1112.
(15) Shahmiri, M.; Ibrahim, N. A.; Shayesteh, F.; Asim, N.; Motallebi, N. Preparation of PVP-Coated Copper Oxide Nanosheets as Antibacterial and Antifungal Agents. *J. Mater. Res.* **2013**, *28*, 3109−3118.
(16) Ahrari, F.; Eslami, N.; Rajabi, O.; Ghazvini, K.; Barati, S. The Antimicrobial Sensitivity of Streptococcus Mutans and Streptococcus Sangius to Colloidal Solutions of Different Nanoparticles Applied as Mouthwashes. *Dent. Res. J.* **2015**, *12*, 44−49.
(17) Ismail, R. A.; Ali, A. K.; Ismail, M. M.; Hassoon, K. I. Preparation and Characterization of Colloidal ZnO Nanoparticles Using Nanosecond Laser Ablation in Water. *Appl. Nanosci.* **2011**, *1*, 45−49.
(18) Beyth, N.; Houri-Haddad, Y.; Domb, A.; Khan, W.; Hazan, R. Alternative Antimicrobial Approach: Nano-Antimicrobial Materials. *J. Evidence-Based Complementary Altern. Med.* **2015**, *2015*, 246012.
(19) Khashan, K. S.; Sulaiman, G. M.; Abdulameer, F. A. Synthesis and Antibacterial Activity of CuO Nanoparticles Suspension Induced by Laser Ablation in Liquid. *Arabian J. Sci. Eng.* **2016**, *41*, 301−310.
(20) Mahapatra, O.; Bhagat, M.; Gopalakrishnan, C.; Arunachalam, K. D. Ultrafine Dispersed CuO Nanoparticles and Their Antibacterial Activity. *J. Exp. Nanosci.* **2008**, *3*, 185−193.
(21) Bondarenko, O.; Juganson, K.; Ivask, A.; Kasemets, K.; Mortimer, M.; Kahru, A. Toxicity of Ag, CuO and ZnO Nanoparticles to Selected Environmentally Relevant Test Organisms and Mammalian Cells in Vitro: A Critical Review. *Arch. Toxicol.* **2013**, *87*, 1181−1200.
(22) Bacchetta, R.; Moschini, E.; Santo, N.; Fascio, U.; Del Giacco, L.; Freddi, S.; Camatini, M.; Mantecca, P. Evidence and Uptake Routes for Zinc Oxide Nanoparticles through the Gastrointestinal Barrier in Xenopus Laevis. *Nanotoxicology* **2014**, *8*, 728−744.
(23) Bonfanti, P.; Moschini, E.; Saibene, M.; Bacchetta, R.; Rettighieri, L.; Calabri, L.; Colombo, A.; Mantecca, P. Do Nanoparticle Physico-Chemical Properties and Developmental Exposure Window Influence Nano ZnO Embryotoxicity in Xenopus Laevis? *Int. J. Environ. Res. Public Health* **2015**, *12*, 8828−8848.
(24) Midander, K.; Cronholm, P.; Karlsson, H. L.; Elihn, K.; Möller, L.; Leygraf, C.; Wallinder, I. O. Surface Characteristics, Copper Release, and Toxicity of Nano- and Micrometer-Sized Copper and Copper(II) Oxide Particles: A Cross-Disciplinary Study. *Small* **2009**, *5*, 389−399.
(25) Moschini, E.; Gualtieri, M.; Colombo, M.; Fascio, U.; Camatini, M.; Mantecca, P. The Modality of Cell-Particle Interactions Drives the Toxicity of Nanosized CuO and TiO2 in Human Alveolar Epithelial Cells. *Toxicol. Lett.* **2013**, *222*, 102−116.
(26) Semisch, A.; Ohle, J.; Witt, B.; Hartwig, A. Cytotoxicity and genotoxicity of nano - and microparticulate copper oxide: role of solubility and intracellular bioavailability. *Part. Fibre Toxicol.* **2014**, *11*, 10.
(27) Perelshtein, I.; Lipovsky, A.; Perkas, N.; Gedanken, A.; Moschini, E.; Mantecca, P. The Influence of the Crystalline Nature of Nano-Metal Oxides on Their Antibacterial and Toxicity Properties. *Nano Res.* **2015**, *8*, 695−707.
(28) Zhang, S.; Gao, H.; Bao, G. Physical Principles of Nanoparticle Cellular Endocytosis. *ACS Nano* **2015**, *9*, 8655−8671.
(29) Lee, Y. K.; Choi, E. J.; Webster, T. J.; Kim, S. H.; Khang, D. Effect of the Protein Corona on Nanoparticles for Modulating Cytotoxicity and Immunotoxicity. *Int. J. Nanomed.* **2015**, *10*, 97−113.
(30) Bastian, S.; Busch, W.; Kühnel, D.; Springer, A.; Meißner, T.; Holke, R.; Scholz, S.; Iwe, M.; Pompe, W.; Gelinsky, M.; et al. Toxicity of Tungsten Carbide and Cobalt-Doped Tungsten Carbide Nanoparticles in Mammalian Cells in Vitro. *Environ. Health Perspect.* **2009**, *117*, 530−536.
(31) Nagvenkar, A. P.; Deokar, A.; Perelshtein, I.; Gedanken, A. A One-Step Sonochemical Synthesis of Stable ZnO−PVA Nanocolloid as a Potential Biocidal Agent. *J. Mater. Chem. B* **2016**, *4*, 2124−2132.
(32) Hojo, N.; Shirai, H.; Hayashi, S. Complex Formation Between Poly(Vinyl Alcohol) and Metallic Ions in Aqueous Solution. *J. Polym. Sci.* **1974**, *47*, 299−307.
(33) Eliseev, A. A.; Lukashin, A. V.; Vertegel, A. A.; Heifets, L. I.; Zhirov, A. I.; Tretyakov, Y. D. Complexes of Cu (II) with Polyvinyl Alcohol as Precursors for the Preparation of CuO/SiO_2 Nanocomposites. *Mater. Res. Innovations* **2000**, *3*, 0308−0312.
(34) Applerot, G.; Lellouche, J.; Lipovsky, A.; Nitzan, Y.; Lubart, R.; Gedanken, A.; Banin, E. Understanding the Antibacterial Mechanism of CuO Nanoparticles: Revealing the Route of Induced Oxidative Stress. *Small* **2012**, *8*, 3326−3337.
(35) Applerot, G.; Lipovsky, A.; Dror, R.; Perkas, N.; Nitzan, Y.; Lubart, R.; Gedanken, A. Enhanced Antibacterial Activity of Nanocrystalline ZnO Due to Increased ROS-Mediated Cell Injury. *Adv. Funct. Mater.* **2009**, *19*, 842−852.
(36) Chang, Y.-N.; Zhang, M.; Xia, L.; Zhang, J.; Xing, G. The Toxic Effects and Mechanisms of CuO and ZnO Nanoparticles. *Materials* **2012**, *5*, 2850−2871.
(37) Ray, P. D.; Huang, B.-W.; Tsuji, Y. Reactive Oxygen Species (ROS) Homeostasis and Redox Regulation in Cellular Signaling. *Cell. Signalling* **2012**, *24*, 981−990.
(38) Hayyan, M.; Hashim, M. A.; AlNashef, I. M. Superoxide Ion: Generation and Chemical Implications. *Chem. Rev.* **2016**, *116*, 3029−3085.
(39) Li, Y.; Zhang, W.; Niu, J.; Chen, Y. Mechanism of Photogenerated Reactive Oxygen Species and Correlation with the Antibacterial Properties of Engineered Metal-Oxide Nanoparticles. *ACS Nano* **2012**, *6*, 5164−5173.
(40) Kohno, M. Applications of Electron Spin Resonance Spectrometry for Reactive Oxygen Species and Reactive Nitrogen Species Research. *J. Clin. Biochem. Nutr.* **2010**, *47*, 1−11.
(41) Schiek, M.; Al-Shamery, K.; Kunat, M.; Traeger, F.; Wöll, C. Water Adsorption on the Hydroxylated H-(1×1) O-ZnO(0001) Surface. *Phys. Chem. Chem. Phys.* **2006**, *8*, 1505−1512.
(42) Tabah, B.; Nagvenkar, A. P.; Perkas, N.; Gedanken, A. Solar-Heated Sustainable Biodiesel Production from Waste Cooking Oil Using a Sonochemically Deposited SrO Catalyst on Microporous Activated Carbon. *Energy Fuels* **2017**, *31*, 6228−6239.
(43) Fu, P. P.; Xia, Q.; Hwang, H.-M.; Ray, P. C.; Yu, H. Mechanisms of nanotoxicity: Generation of reactive oxygen species. *J. Food Drug Anal.* **2014**, *22*, 64−75.
(44) Kafil, V.; Omidi, Y. Cytotoxic Impacts of Linear and Branched Polyethylenimine Nanostructures in A431 Cells. *Bioimpacts* **2011**, *1*, 23−30.

DOI: 10.1021/acsomega.9b00181
ACS Omega 2019, 4, 13631−13639

(45) Nguyen, J.; Xie, X.; Neu, M.; Dumitrascu, R.; Reul, R.; Sitterberg, J.; Bakowsky, U.; Schermuly, R.; Fink, L.; Schmehl, T.; et al. Effects of Cell-Penetrating Peptides and Pegylation on Transfection Efficiency of Polyethylenimine in Mouse Lungs. *J. Gene Med.* **2008**, *10*, 1236−1246.
(46) Li, Y.; Kröger, M.; Liu, W. K. Endocytosis of PEGylated Nanoparticles Accompanied by Structural and Free Energy Changes of the Grafted Polyethylene Glycol. *Biomaterials* **2014**, *35*, 8467−8478.
(47) Sanchez, L.; Yi, Y.; Yu, Y. Effect of Partial PEGylation on Particle Uptake by Macrophages. *Nanoscale* **2017**, *9*, 288−297.
(48) Suk, J. S.; Xu, Q.; Kim, N.; Hanes, J.; Ensign, L. M. PEGylation as a Strategy for Improving Nanoparticle-Based Drug and Gene Delivery. *Adv. Drug Delivery Rev.* **2016**, *99*, 28−51.
(49) Guaiquil, V. H.; Vera, J. C.; Golde, D. W. Mechanism of Vitamin C Inhibition of Cell Death Induced by Oxidative Stress in Glutathione-Depleted HL-60 Cells. *J. Biol. Chem.* **2001**, *276*, 40955−40961.
(50) Ndiaye, M. A.; Nihal, M.; Wood, G. S.; Ahmad, N. Skin, Reactive Oxygen Species, and Circadian Clocks. *Antioxid. Redox Signaling* **2014**, *20*, 2982−2996.
(51) Bouzas, V.; Haller, T.; Hobi, N.; Felder, E.; Pastoriza-Santos, I.; Pérez-Gil, J. Nontoxic Impact of PEG-Coated Gold Nanospheres on Functional Pulmonary Surfactant-Secreting Alveolar Type II Cells. *Nanotoxicology* **2014**, *8*, 813−823.
(52) Alcantar, N. A.; Aydil, E. S.; Israelachvili, J. N. Polyethylene Glycol-Coated Biocompatible Surfaces. *J. Biomed. Mater. Res.* **2000**, *51*, 343−351.
(53) Mihai, C.; Chrisler, W. B.; Xie, Y.; Hu, D.; Szymanski, C. J.; Tolic, A.; Klein, J. A.; Smith, J. N.; Tarasevich, B. J.; Orr, G. Intracellular Accumulation Dynamics and Fate of Zinc Ions in Alveolar Epithelial Cells Exposed to Airborne ZnO Nanoparticles at the Air-Liquid Interface. *Nanotoxicology* **2015**, *9*, 9−22.
(54) Shen, C.; James, S. A.; de Jonge, M. D.; Turney, T. W.; Wright, P. F. A.; Feltis, B. N. Relating Cytotoxicity, Zinc Ions, and Reactive Oxygen in ZnO Nanoparticle-Exposed Human Immune Cells. *Toxicol. Sci.* **2013**, *136*, 120−130.

DOI: 10.1021/acsomega.9b00181
ACS Omega 2019, 4, 13631−13639